JOURNAL OF CATALYSIS **166,** 25–35 (1997)
ARTICLE NO. CA971494

Structure Sensitivity of the Hydrogenation of Crotonaldehyde over Pt/SiO_2 and Pt/TiO_2

Martin Englisch,* Andreas Jentys,† and Johannes A. Lercher*,[1]

*Department of Chemical Technology, University of Twente, P.O. Box 217, 7500AE Enschede, The Netherlands; and †Institut für Physikalische Chemie, Technische Universität Wien, Getreidemarkt 9, A-1060 Wien, Austria

Received March 6, 1996; revised October 15, 1996; accepted October 16, 1996

Hydrogenation of crotonaldehyde has been studied over SiO_2- and TiO_2-supported Pt catalysts. Over Pt/SiO_2, the selectivity to the primary products butyraldehyde and crotylalcohol depends critically on the Pt particle size; i.e., the selectivity to the unsaturated alcohol increases with increasing particle size. For large metal particles, the high fraction of Pt(111) surfaces is concluded to favor the adsorption of crotonaldehyde via the carbonyl bond. On small Pt particles, the high abundance of metal atoms in low coordination allows unconstrained adsorption of both double bonds. In this case, the hydrogenation of the C=C bond is kinetically favored. Activity and selectivity of Pt/TiO_2 catalysts after low-temperature reduction are similar to those of Pt/SiO_2. After high-temperature reduction the selectivity to crotylalcohol is generally enhanced. The selectivity of Pt/TiO_2 catalysts is then determined by the metal particle size and the extent of decoration of Pt with TiO_x particles. The presence of coordinatively unsaturated Ti cations in these oxide particles enhances the sorption strength of the C=O bond resulting in an enhanced selectivity to crotylalcohol. The effects of metal particle size and promotion by TiO_x are additive. TiO_x promotion of catalysts with small particles and the presence of unpromoted large particles allow reaching of selectivities to crotylalcohol of approximately 45%. Promotion of large Pt particles with TiO_x yields 64% selectivity to crotylalcohol.

1. INTRODUCTION

Hydrogenation of α,β-unsaturated aldehydes lead to two primary reaction products: the saturated aldehyde and the unsaturated alcohol (see Fig. 1). For small molecules like acrolein and crotonaldehyde, the reaction to the saturated aldehyde is thermodynamically and kinetically favored (1, 2), while for larger α,β-unsaturated aldehydes additional steric constraints imposed by the substituents on the C=C double bond might influence the product selectivity. The development and characterization of catalysts for the selective hydrogenation of α,β-unsaturated aldehydes with special emphasis on cinnamaldehyde has been recently reviewed by Gallezot *et al.* (3). Promoted and unpromoted metals (4, 5, 6) and various supports (carbon based (7), metal oxide (8), and microporous (9) supports) have been explored in that respect. Despite the thorough investigation of the influence of the chemical nature of the metal on the selectivity the role of the particle size effects has seen less attention. Only in one example was it shown that the particle size of ruthenium catalysts influenced the selectivity in cinnamaldehyde hydrogenation (6, 10, 11). For the hydrogenation of acrolein this effect was not observed (4).

Theoretical calculations (12) and studies on single crystals (13) indicate that the sorption structure of α,β-unsaturated aldehydes subtly depends on the exposed metal surface planes and the substituents at the C=C bond. Delbecq *et al.* (12) estimated the binding energies for selected α,β-unsaturated aldehydes using semi-empirical extended Hückel calculations. The results suggest that unsaturated aldehydes adsorb preferentially in a planar η_4 adsorption form on Pt(100) surfaces and in a π_{CC} form on Pt(110) and on surface steps (see Fig. 2). For Pt(111), only acrolein seems to be preferentially sorbed in a di-σ_{CC} mode, while crotonaldehyde and cinnamaldehyde are sorbed in a di-σ_{CO} mode. If the selectivity in the catalytic hydrogenation is related to the sorption structure, the differences suggest that the selectivity to the unsaturated alcohol (except for acrolein) might be influenced by the fraction of Pt(111) surface planes exposed. This fraction increases with the size of the metal particles (14) and, thus, the selectivity to the unsaturated alcohol should as well increase with the particle size.

In the present contribution we aim to separate these particle size effects from the effects of chemical promotion for the selectivity in the hydrogenation of crotonaldehyde. Pt catalysts supported on SiO_2 and TiO_2 are compared. For both series of catalysts a sequence of samples has been prepared exhibiting different dispersions. In the case of Pt/TiO_2, the reversible strong metal support interaction (SMSI) induced decoration of Pt particles with titania suboxides is utilized to induce chemical promotion without changing the metal particle size of the Pt catalyst. This

[1] To whom correspondence should be addressed.

0021-9517/97 $25.00

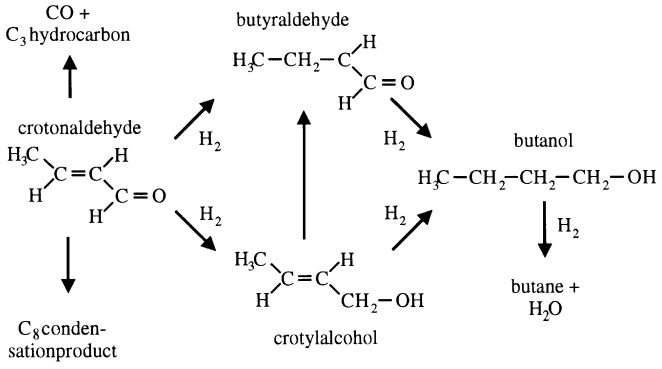

FIG. 1. Reaction scheme of crotonaldehyde.

produces results similar to base metal oxide promoted catalysts (8, 9).

2. EXPERIMENTAL

2.1. Catalyst Preparation

Silica-supported Pt catalysts are grouped according to their pretreatment. Series A consists of five catalysts: the EURO-Pt 1 (A1, having 6.3 wt% Pt, prepared by ion exchange with a $Pt(NH_3)_4Cl_2$ solution (15)), three catalysts prepared by ion exchange using an aqueous $Pt(NH_3)_4(OH)_2$ solution (A2, A3, and A5 with a metal loading of 2, 3.2, and 4 wt% Pt, respectively), and one catalyst prepared by impregnation with chloroplatinic acid (A4, 4 wt%). The dried precursors of series A were calcined in flowing air and reduced in flowing hydrogen at 673 K for 1 h. Pt/SiO_2 catalysts of series B were derived from catalyst A5 by extended reduction to obtain catalysts with large Pt particles. Catalyst B1 was obtained by reduction in flowing hydrogen for 7 h at 673 K and catalyst B2 by reduction for 3 h at 1073 K. Pt catalysts supported on TiO_2 (series C) were prepared by ion exchange (C1, 2 wt% Pt) and impregnation (C2 and C3, 7 wt% Pt). TiO_2 supported catalysts were not prereduced.

2.2. Catalyst Characterization

The metal dispersion of the catalysts was derived from hydrogen chemisorption measurements performed in an all glass volumetric adsorption system. The particle size distribution of selected catalysts was studied by transmission electron microscopy (TEM) using a Philips CM 30 microscope (300 kV). All particles visible on the TEM photographs were evaluated and classified using the equivalent circle diameter and the average diameter presented is determined as the mean diameter according to Ref. (16). EDAX measurements of the reduced catalysts confirmed the absence of impurities (i.e., residual chlorine from the catalyst precursors).

2.3. X-Ray Absorption Spectroscopy

The X-ray absorption spectroscopy measurements were performed at the NSLS, Brookhaven National Laboratory, Upton, NY, beamline X23A2 equipped with a Si(311) double crystal monochromator that required no detune and at the Synchrotron of the Cornell University, Cornell, NY, beamline C2 equipped with a Si(220) double crystal monochromator detuned to 50% intensity. Catalysts were pressed into self-supporting wafers and placed in a stainless steel chamber, reduced at the desired temperature and investigated *in situ* (see Refs. (17, 18)). Spectra were recorded at liquid N_2 temperature after consecutive reduction in 5% H_2 in He at 473, 673, 773, and 873 K for 90 min. The EXAFS analysis followed standard procedures. The k^2-weighted spectra were Fourier transformed within the limits $k = 3.5$ to $k = 18$ (18). The EXAFS of a selected shell were fitted using phase-shift and amplitude functions obtained from reference compounds (Pt-foil, PtO_2) under the assumption of plane waves and single scattering. Note that the absolute error of coordination numbers obtained from X-ray absorption spectroscopy is ± 0.5, but the relative error in the consecutive experiments in the fixed experimental setup was found to be approximately ± 0.1.

2.4. Infrared Spectroscopy

A Bruker IFS-88 spectrometer was used for the IR-measurements. The catalysts were pressed into self-supporting wafers and placed in a stainless steel chamber (with characteristics of a CSTR reactor) that allowed to follow the reduction, sorption, and hydrogenation of probe molecules *in situ*. During reaction, samples of the reactor effluent were taken and at the same time infrared spectra of the catalyst were recorded (time resolution 20 s, spectral resolution 4 cm^{-1}). The gas samples from the reactor were stored in the sample loops of a multiport valve and analyzed subsequently by gaschromatography.

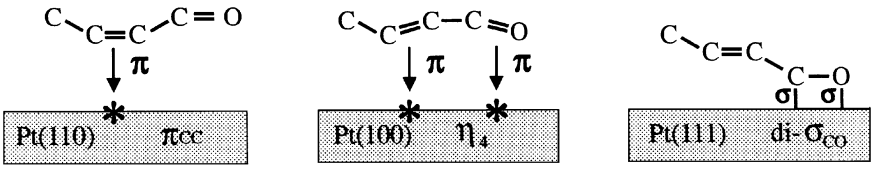

FIG. 2. Proposed sorption structures of crotonaldehyde on Pt according to Ref. (12).

2.5. Hydrogenation Experiments

Gas-phase hydrogenation of crotonaldehyde (CrHO), butyraldehyde (BuHO), and crotylalcohol (CrOH) was carried out in a tubular quartz glass reactor under atmospheric pressure as described in Ref. (19). All catalysts were rereduced *in situ* in pure hydrogen before the experiments at 673 K for at least 30 min. Reactants were introduced by a saturator and/or a syringe pump to obtain partial pressures between 16 and 60 mbar for the reactant and 1084 and 1040 mbar for H_2. The conversion was kept below 10%. The reaction temperature was 353 K. As the catalysts deactivated during reaction, all results of the hydrogenation of crotonaldehyde in the gas phase are reported after 90 min on stream.

Hydrogenation of crotonaldehyde in liquid phase was performed in stirred autoclaves (volume 65 ml). The reactants (1 ml CrHO, 1 ml H_2O and 8 ml ethanol) and the catalyst were introduced into the autoclave. Then, the reactor was purged extensively with He and pressurized with pure H_2 to 25 bar. The reaction was carried out at room temperature (~300 K). After approximately 50% conversion, the autoclaves were opened and the catalyst was separated from the reaction mixture by a micro filter attached to the syringe used for sampling.

The composition of the samples of both gas- and liquid-phase experiments were analyzed by gas chromatography using a HP5890 gas chromatograph equipped with a 30 m J&W DB-WAX capillary column and a FID detector.

3. RESULTS

3.1. Catalyst Characterization

Pt supported on SiO_2. The dispersion (H/Pt ratio) and the average metal particle size of the catalysts are summarized in Table 2. TEM photographs of the ion-exchanged catalysts (A1 (15), A2, and A5) show uniform spherical metal clusters with a relatively narrow particle size distribution. The same average diameters measured for catalyst A1 (15) and for catalyst A2 (1.8 nm) and the same H/Pt ratio of 1 for both catalysts suggest a similar average particle size of these two samples consisting of approximately 30 metal atoms per particle. The average diameter of the metal particles of catalyst A5 was 2.3 nm, the H/Pt ratio was 0.75. This suggests that the particles consist of approximately 60 metal atoms. The sintered catalyst B2 shows a bimodal particle size distribution consisting of small (around 2.3 nm) and quite large (around 17 nm) metal particles. Bimodal particle size distributions may occur upon sintering, see Ref. (20).

The XANES of all silica supported samples indicate complete reduction in hydrogen above 453 K. As an example the XANES recorded during reduction of catalyst A2 are shown in Fig. 3. The maximum in the change of the intensity (or height) of the white line occurs in parallel to the maximum in the hydrogen consumption. For details of the experimental method see Ref. (18).

Pt supported on TiO_2. TEM photographs of the highly dispersed Pt/TiO_2 catalyst (C1) showed a narrow particle size distribution with particles of around 1 nm. Pt on TiO_2 prepared by incipient wetness (C3) consisted of larger metal clusters and a relatively wide particle size distribution (mean diameter 12 nm). The average metal particle size of all catalysts was determined by EXAFS and hydrogen chemisorption at different reduction temperatures. These results are compiled in Table 1.

The XANES of the catalysts C2 and C3 at all and that of catalyst C1 at low reduction temperatures were identical to the XANES of the Pt reference foil. Pt–O coordinations

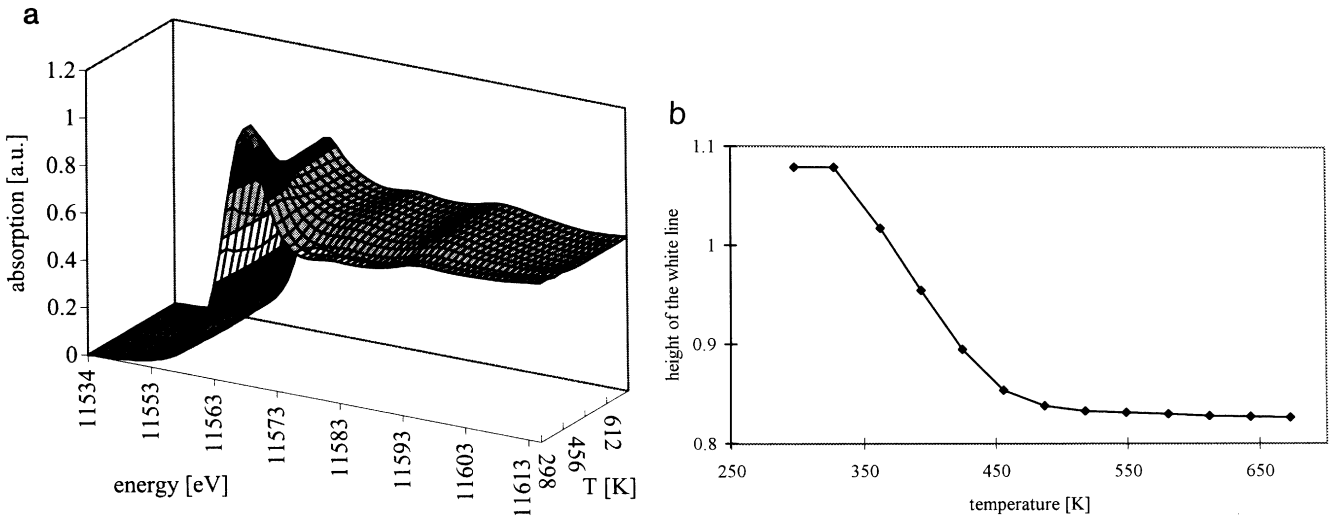

FIG. 3. (a) XANES of the Pt L_{III} edge of catalyst A2 during reduction (heating rate 10 K/min, time resolution: 2 min), (b) Height of the white line as a function of the reduction temperature.

TABLE 1

Average First Shell Coordination Number (N) and H/Pt Ratios for Pt/TiO_2 Catalysts

	Reduced at 473 K		Reduced at 673 K		Reduced at 873 K	
	N	H/Pt	N	H/Pt	N	H/Pt[a]
C1 (IE)	<4	1.0	<4	0.40	<4	0.27
C2 (IW)	8.3	0.30	8.5	0.042	8.5	0.027
C3 (IW)	8.7	0.22	9	0.035	9	0.020

Note. IW: prepared by impregnation; IE: prepared by ion exchange.
[a] H/Pt ratio was measured after rereduction at 773 K due to experimental limitation.

were not found in the EXAFS indicating full reduction of Pt. The EXAFS of the ion-exchanged catalyst C1 suggests the presence of very small metal particles consisting of only a few metal atoms ($N < 4$) for all reduction temperatures. The analysis of the X-ray absorption spectra of the two impregnated samples (C2, C3) indicates some dependence of the particle size on the reduction temperature. Upon reduction at 473 and 673 K a slight increase in the Pt–Pt coordination number of the first shell was found (see Table 1). After reduction at 873 K, the same coordination number as after reduction at 673 K was observed. Thus, we conclude that the Pt particles did not sinter between 623 and 873 K in hydrogen atmosphere. In comparable measurements of Pt/SiO_2 catalysts increased sintering with rising reduction temperatures was found. To probe for the effect of hydrogen upon sintering of the Pt particles at high reduction temperatures, catalyst C2 was heated in He atmosphere to avoid reduction of the support (see Fig. 4). EXAFS analysis indicates again fully reduced Pt at 473 K (decomposition of the precursor) and yields approximately the same coordination number as for the corresponding sample reduced

TABLE 2

Arithmetic Mean Diameter of the Metal Particles, H/Pt Ratio, Activity (TOF) for a Reaction Temperature of 353 K, and Selectivities to the Primary Products for the Gas Phase Hydrogenation over Pt/SiO_2 Catalysts

		Average diameter (nm)	H/Pt ratio	TOF ($^{-s}$)	Selectivity to BuHO (mol%)	Selectivity to CrOH (mol%)
EURO-Pt 1 (IE)	A1	1.8 (15)	1	0.015	83	8
Pt/SiO_2 (IE)	A2	1.8	1	0.015	90	5
Pt/SiO_2 (IE)	A3	n.d.	0.75	0.012	74	15
Pt/SiO_2 (IW)	A4	n.d.	0.45	0.021	60	23
Pt/SiO_2 (IE)	A5	2.3	0.72	0.012	76	15
Pt/SiO_2	B1	n.d.	0.64	0.016	48	34
Pt/SiO_2	B2	2.3 and 1.7	0.25	0.070	42	43

Note. IW: prepared by impregnation; IE: prepared by ion exchange; n.d.: not detected. TOF [molecules converted/accessible site, s].

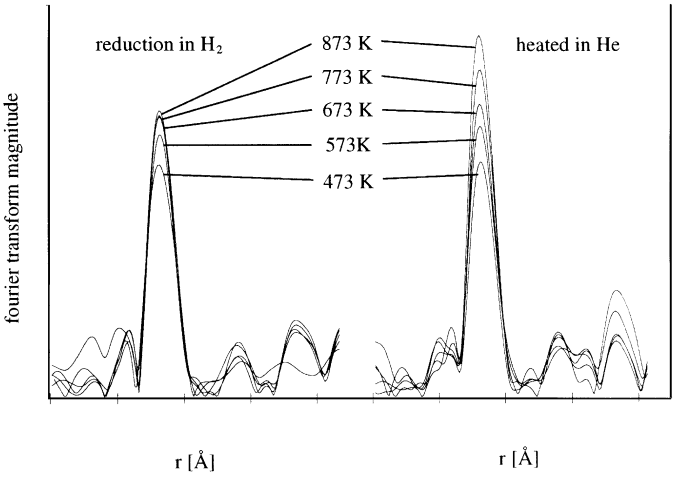

FIG. 4. Fourier transforms of catalyst C3 (Pt/TiO_2) of the k^2 weighted EXAFS for reduction in hydrogen and heating in He at the temperatures indicated.

in hydrogen. However, the average coordination number increased steadily with increasing reduction temperature (8.3, 9.8, 10.2, and 10.8 for 473, and 573, 673, and 773 K in He, respectively).

3.2. Hydrogenation of Crotonaldehyde

Pt supported on SiO_2. The turnover frequency and the selectivities to the primary products crotylacohol and butyraldehyde for the hydrogenation of crotonaldehyde over Pt/SiO_2 catalysts are compiled in Table 2. The secondary reactions to butanol and C_4 hydrocarbons and decarbonylation to CO and C_3 hydrocarbons account for the difference to 100% in the tables. For all Pt/SiO_2 catalysts the selectivity to the unsaturated alcohol increased with decreasing dispersion. For catalysts with small particles (A1–A3, A5, and B1) a clear trend of the catalyst activity as a function of dispersion was not found. However, the highest activity was observed for the catalysts with large particles (A4 and B2).

Since all catalysts deactivated substantially during the hydrogenation of crotonaldehyde the results are reported after 90 min on stream and at a similar conversion. The deactivation can be separated into two regimes. During the first 20 min on stream the catalysts deactivate extremely fast. That period is followed by a logarithmic deactivation investigated up to 48 h (Fig. 5). *In situ* IR spectra of the catalysts during reaction showed fast increasing surface concentrations of CO (linearly bound CO at approximately 2030 cm^{-1} (21)) for the first 20 min on stream, shown for samples A2 in Fig. 6. The band of the C=O stretching vibration at ~1720 cm^{-1}, assigned to the carbonyl group of crotonaldehyde adsorbed at the silanol groups of the support, increased with time on stream. The conversion decreased in parallel with increasing concentrations of adsorbed CO (see Fig. 7). CO is irreversibly adsorbed under the reaction

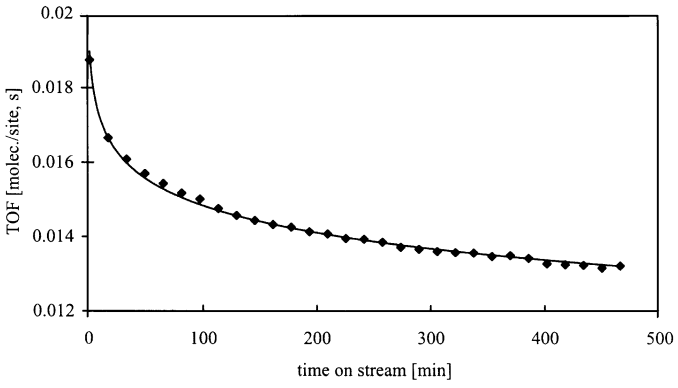

FIG. 5. TOF as a function of time on stream for catalyst A2 (reaction temperature 353 K).

conditions used. Reduction or evacuation at 673 K removes the sorbed CO completely and the initial activity can be restored. Note that the conversion decreases by a logarithmic function as shown in Fig. 5.

The bands at 2968, 2942, 2913, and 2882 cm^{-1} were assigned to stretching vibrations of CH_2 and CH_3 groups, indicating the presence of relatively long organic molecules. These organic molecules could only partially be removed by purging with He or by hydrogenation at 673 K. The incomplete regeneration of the silanol groups upon these treatments indicates that at least a part of these organic residues interact with the silanol groups of the support. The presence of these species apparently did not influence the activity of the catalyst, but possibly the selectivity (22).

The selectivity to hydrocarbons decreased from more than 80% at 20 s on stream to less than 10% after 20 min on stream. Note that the hydrocarbons could not be analyzed in detail due to limitations of the GC column used. Their concentration was calculated assuming that butane

TABLE 3

H/Pt Ratio, Activity (Integral TON after 960 Min Reaction Time at ~300 K) and Selectivity to the Primary Products Butyraldehyde (S_{BuHO}) and Crotylalcohol (S_{CrOH}) in Liquid Phase for a Conversion of ~50%

		H/Pt ratio	Activity (integral TON)	S_{BuHO} (mol%)	S_{CrOH} (mol%)
Pt/SiO_2	A2	1.0	640	65	17
Pt/SiO_2	B1	0.64	750	49	35
Pt/SiO_2	B2	0.25	1500	44	41

Note. TON (molecules converted/accessible metal atom).

was the only product. The selectivity to the primary product butyraldehyde increased significantly during the first 2 min on stream and seemed to reach a steady state after approximately 15 min on stream. The selectivity to the other primary product, crotylalcohol, increased steadily until the end of the experiments after 20 min reaction time. The selectivity to the secondary product butanol passed a maximum at approximately 2 min on stream. The rate decreased by some 80% in this first 20 min and in parallel the concentration of adsorbed CO increased.

In liquid phase, hydrogenation ceased after a certain number of turnovers, the composition of the liquid phase as a function of time is shown in Fig. 8 for catalyst A3. The activity of the catalysts was compared by the integral turnover number (TON) for a defined reaction time since the composition of the liquid phase did not change when the catalysts lost their activity and meaningful rates could not be calculated because of the deactivation. The TON compiled in Table 3 were obtained for catalysts that practically lost their activity. The product distribution of the hydrogenation in liquid phase showed similar trends as observed

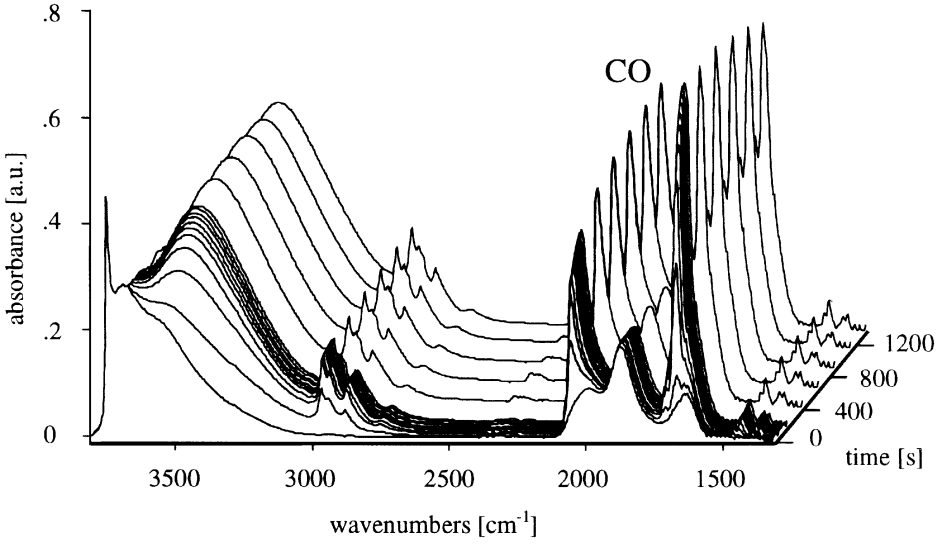

FIG. 6. IR spectra of catalyst A2 during the first 20 min of the hydrogenation of crotonaldehyde.

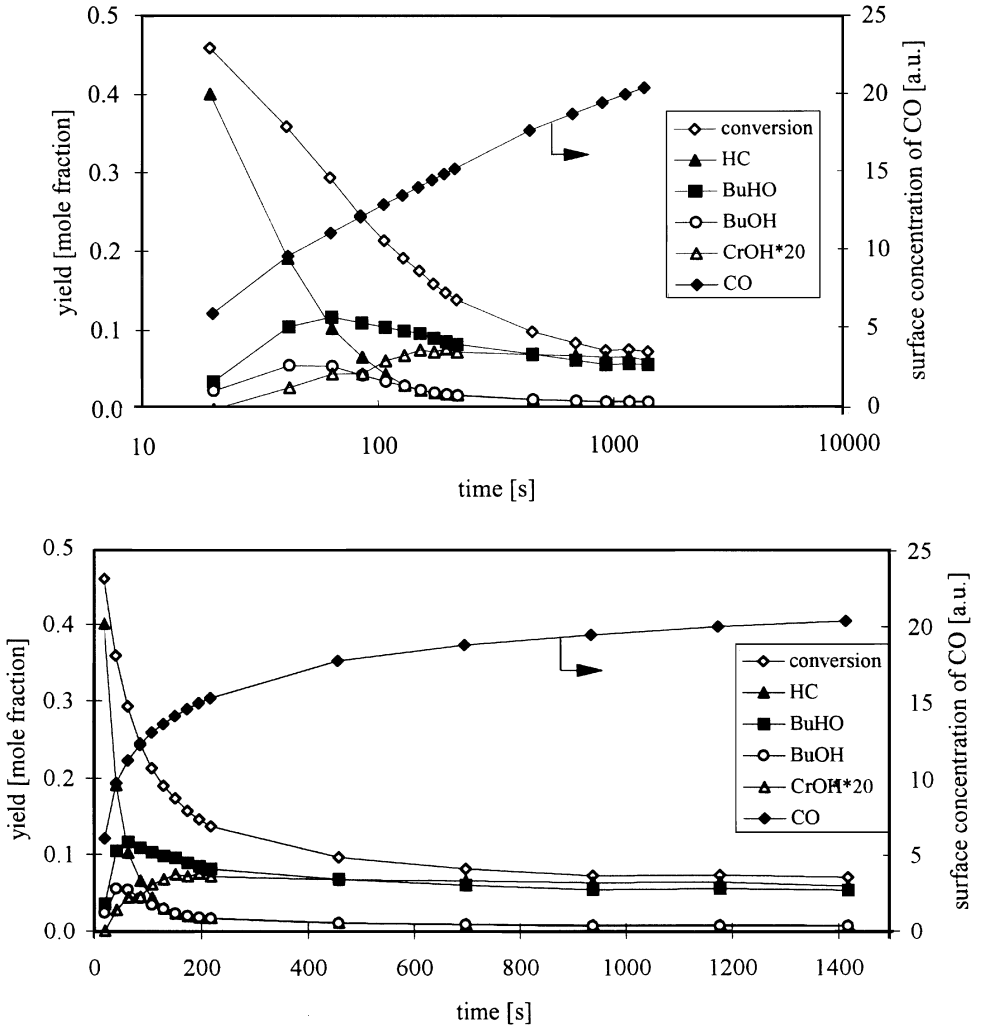

FIG. 7. Conversion, yields of the hydrogenation of crotonaldehyde over catalyst A2 during the first 20 min on stream and the integrated area of the band at 3100–2800 cm^{-1} attributed to linearly bound CO (secondary axis).

in the gas phase, the selectivity to crotylalcohol increased with increasing metal particle size. In addition, the selectivity to crotylalcohol increased with increasing conversion, the highest yields of crotylacohol were observed for a conversion between 60 and 80%.

Pt supported on TiO_2. The results of the gas phase hydrogenation of crotonaldehyde over Pt/TiO_2 catalysts are compiled in Table 4 for three different pretreatment temperatures, i.e., low-temperature reduction (1 h at 473 K), high-temperature reduction (1 h at 773 K), and reduction–oxidation–reduction cycle (reduction 2 h at 773, calcination 2 h at 673 K, rereduction 1 h at 473 K).

The activity and the selectivity of the catalysts increased with increasing metal particle size. The TOF increased by an order of magnitude after the first high-temperature reduction, but stayed nearly constant upon further reduction–oxidation–reduction cycles (Fig. 9).

In liquid-phase hydrogenation the selectivity to the unsaturated alcohol was 11% for the catalyst with the smallest metal particles (C1) and 33% for the catalyst with the largest metal particles (C3). The activity of both catalysts

TABLE 4

Average First Shell Coordination Number (N), Activity (TOF) for a Reaction Temperature of 353 K and the Selectivity to Crotylalcohol (S_{CrOH}) in the Gas-Phase Hydrogenation over Pt/TiO_2

		Reduction at 473 K		Reduction at 773 K		Reduction–oxidation–reduction cycle	
Pt/TiO_2	N	TOF	S_{CrOH}	TOF	S_{CrOH}	TOF	S_{CrOH}
C1	>4	0.035	11	0.23	33	0.21	45
C2	8.3	0.045	20	0.42	43	0.32	58
C3	8.7	0.050	41	0.56	43	0.46	64

Note. TOF (molecules converted/accessible site, s).

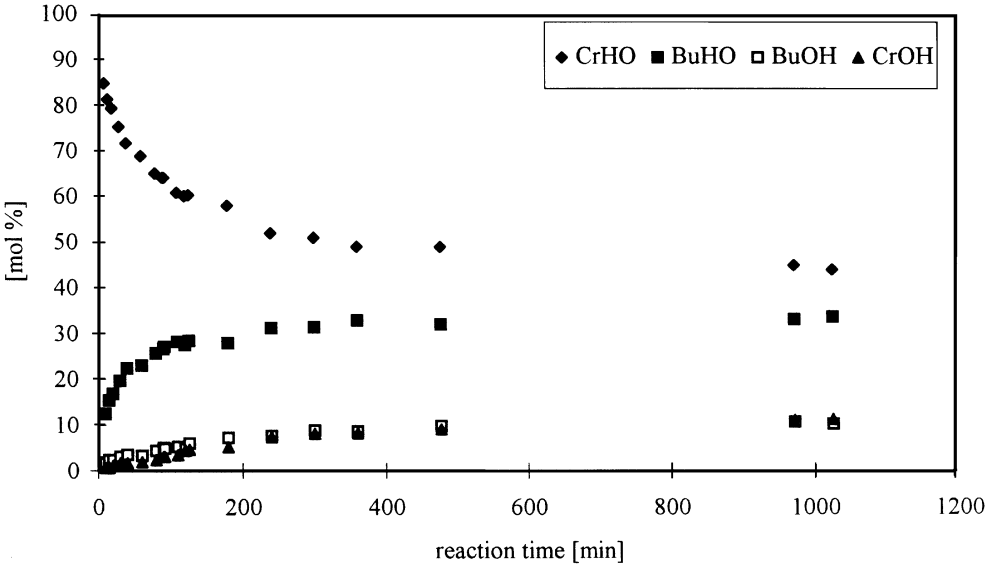

FIG. 8. Hydrogenation of crotonaldehyde in liquid phase over catalyst A3 ($T = 298$ K, solvent = ethanol).

indicated a similar trend as observed for the silica-supported catalysts in liquid phase, the catalyst with the small particles had an integral turnover number of approximately 700 before complete loss of activity, while the catalyst with the largest particles made approximately 1200 turnovers under similar reaction conditions.

4. DISCUSSION

4.1. Physicochemical Properties of Pt Supported on SiO_2 and TiO_2

For silica-supported catalysts a good agreement of the particle size derived from TEM, hydrogen chemisorption, and EXAFS analysis was found for all reduction temperatures. This indicates that the particles are fully accessible (at least for hydrogen). In combination with the generally weak interactions between silica and transition metal particles, variations in the catalytic behavior as discussed below can be related unequivocally to metal particle properties.

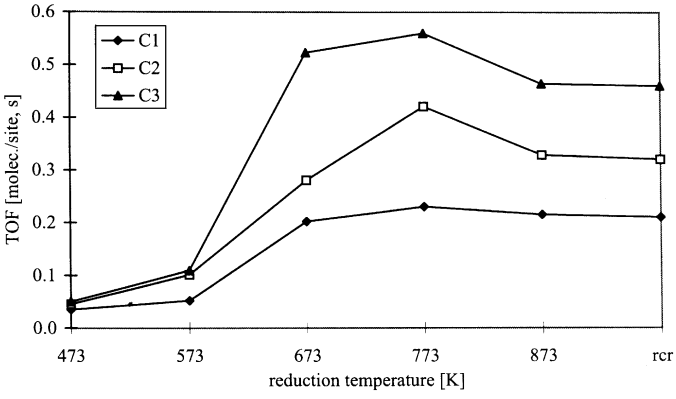

FIG. 9. Activity of the titania supported catalysts as a function of the reduction temperature (rcr = reduction at 773 K, oxidation at 673 K, and rereduction at 673 K cycle).

In contrast, titania is known to influence the sorptive and catalytic properties of Pt catalysts especially after reduction at elevated temperature (1). Hydrogen chemisorption is suppressed for catalysts reduced at elevated temperatures due to the strong metal support interactions (SMSI) (1, 2). Thus, EXAFS analysis of the titania-supported catalysts was used to calculate the metal particle size (23). The use of the average coordination number for determining particle sizes excludes possible errors made in the interpretation of chemisorption results. The smallest metal particles were found with the ion-exchanged sample (C1) where every metal particle consisted of less than 10 atoms (coordination number <4). This is in agreement with the H/Pt ratio of 1 and the narrow particle size distribution of approximately 1 nm found by TEM, measured after low-temperature reduction (473 K). Catalyst C2 (prepared by impregnation) showed a coordination number of 8.3 and a H/Pt ratio of 0.3. Assuming cubooctahedral particle shape its average metal particle is concluded to consist of a few hundred atoms. The formation of small regular crystal planes is possible for this catalyst but edges, corners, and crystal defects are still high in concentration. Catalyst C3 (also prepared by impregnation) consists of large metal particles. A coordination number of 8.7 and a H/Pt ratio of 0.22 suggest metal particles consisting of more than 1000 atoms. For such large metal particles edges and corners are of lesser importance and the Pt(111) surface will be dominating.

After reduction at elevated temperature titania is partially reduced and forms titania suboxides (24–26) that

decorate the metal particles (SMSI state). The lack of significant Pt–O or Pt–Ti backscattering in the EXAFS of the catalysts reduced at 773 and 873 K indicates that regular Pt–O or Pt–Ti coordinations do not exist. In agreement with the results of Short *et al.* (27), the titania suboxides are, thus, concluded to form a disordered overlayer on the Pt particles. The minor decrease in the white line for the catalyst with the smallest particle after reduction at elevated temperatures is tentatively attributed to a particle size effect (28). Note that the decrease in the white line would also be compatible with a transfer of electrons from TiO_x to the metal (29). The change of the white line intensity is, however, negligible for samples with larger metal particles where only a minor fraction of the Pt atoms is located at the surface.

4.2. *Hydrogenation of Crotonaldehyde over Pt/SiO$_2$*

The results show a marked dependence of the selectivity to butyraldehyde and crotylalcohol upon the metal particle size (see Table 2). These results suggest that the hydrogenation of crotonaldehyde is structure sensitive.

The question arises now, if the selectivity of monometallic Pt catalysts depends on a specific local arrangement of the surface atoms in different crystallographic positions or on the density of surface planes and the fraction of highly exposed metal atoms.

Previously, it was shown that the selectivity over supported PtNi catalysts is determined by the fraction of bimetallic sites at the surface that activates the C=O bond of crotonaldehyde and, thus, increase the rate of hydrogenation of this bond (19). However, such polar sites cannot be visualized for Pt/SiO_2 catalysts. Moreover, the similar catalytic properties found for Pt/SiO_2 and for Pt/TiO_2 after low-temperature reduction suggests that polar sites possibly generated at the metal/support interface do not contribute markedly to the reaction over these catalysts.

It is known that complex polar molecules assume different sorption structures on the various surface planes and on highly exposed metal atoms such as those in steps and kinks. When crotonaldehyde is adsorbed on small Pt particles, the decrease in the electron density of the *d*-orbitals of Pt suggests that both double bonds interact with the Pt particle (17). If both double bonds are sorbed on the metal surface hydrogenation of the olefinic bond is kinetically favored (12). The rates of hydrogenation of butyraldehyde and crotylalcohol to butanol over such small Pt particles indeed indicate that the rate of the hydrogenation of the olefinic bond is five times faster than the rate of the hydrogenation of the carbonyl group (Table 5). Since XANES results show that both double bonds interact with the same strength, we conclude that the differences in the rates of hydrogenation are not caused by variations in the adsorption constant. Thus, we would like to explain the high selectivity to butyraldehyde with the prevailence of crotonaldehyde molecules adsorbed via both double bonds on highly exposed metal atoms and the then resulting preference of C=C bond hydrogenation. Additionally the yield of crotylalcohol is slightly diminished by isomerization of crotylalcohol to butyraldehyde (see Table 5).

TABLE 5

TOF (Molecules Converted/site, *s*) and Selectivities (%) in the Hydrogenation of Butyraldehyde and Crotylalcohol over Catalyst B1, Reaction Temperature 353 K

Reactant	TOF	S_{HC}	S_{BuOH}	S_{BuOH}	S_{CrOH}
BuHO	0.0057	11	—	88	0
CrOH	0.027	12	9	78	—

In order to discuss the specific sorption structures on the various low-index surface planes, results from single crystal studies and theoretical calculations shall be used (13, 14). In an elegant piece of work Beccat *et al.* (13) showed that Pt(111) exhibit some selectivity to crotylalcohol, while the other low-index surfaces did not. The fact that the preference is not spectacular may be explained with the fact that low crotonaldehyde concentrations always shift the selectivity in the direction of butyraldehyde (30). The theorectical calculations of Delbeq *et al.* (12) suggest that the planar sorption structure (see Fig. 2) involving the interaction with both double bonds is energetically most favored on Pt(100) and on edges and corners (steps and kinks). On Pt(111) steric constraints, however, seem to induce preferential sorption of crotonaldehyde via the carbonyl group leading to selective hydrogenation of the carbonyl group (see Fig. 2).

To compare these model experiments and the theoretical calculations with the situation expected for supported metal catalysts, assumptions concerning the metal particle morphology were made. For particles consisting of less than 60 atoms (i.e., catalysts A1, A2, and C1) edges and corners are assumed to be most abundant on the surface independently of the actual particle shape. With increasing particle size the fraction of low-index planes increases, while the fraction of highly exposed metal atoms decreases. Figure 10 shows the estimated fraction of Pt(111) surfaces as a function of the particle size assuming cubooctahedral shape (14, 31, 32). The increasing fraction of Pt(111) surfaces with increasing metal particle size parallels the increasing selectivity to crotylalcohol. Thus, we conclude that the selectivity to crotylalcohol is affiliated with the abundance of Pt(111) surfaces.

The strength of adsorption of a given molecule on supported metal catalysts depends critically on the morphology and the size of the metal particle. The heat of adsorption usually increases with decreasing average coordination number of the (surface) metal atoms (33) leading to preferential adsorption at low coordination sites like edges

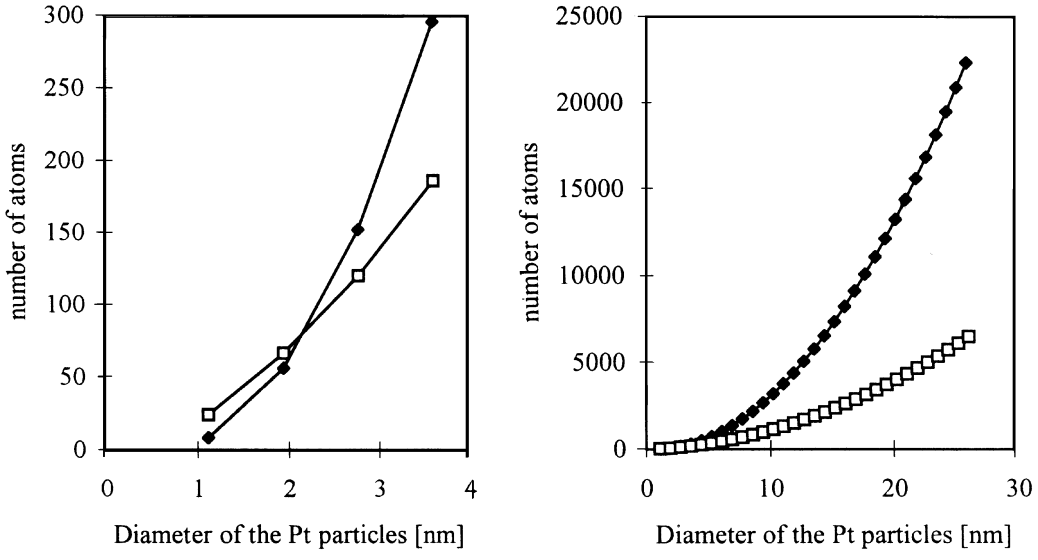

FIG. 10. Exposed surface atoms as a function of the particle size assuming cubooctahedral shape (◆ number of surface atoms in Pt(111) surfaces, □ sum of exposed atoms of other surfaces, edges and corners).

and corners (see, e.g., Ref. (34)). For crotonaldehyde, such strong adsorption may enhance the probability of side reactions like dimerisation and decarbonylation. Since deactivation is caused by decarbonylation and the irreversible adsorption of the generated CO blocking the active metal surface (see also the results of Blackmond *et al.* in Ref. (35)), the lower activity of catalysts with smaller metal particles is attributed to the faster deactivation of the highly exposed surface atoms (see Fig. 7). However, the initial activity of the deactivated catalysts can be restored by evacuation or hydrogenation (36).

The results obtained in the liquid-phase hydrogenation are comparable to those obtained in the gas phase (compare Tables 2 and 3). As observed for gas-phase hydrogenation, the activity and selectivity to crotylalcohol increases with increasing particle size. The results suggest that the surface chemistry observed at low temperatures in the condensed phase is similar to the chemistry observed at elevated temperatures in the gas phase. The lower temperature in the liquid phase, however, cannot prevent deactivation. The deactivation is again attributed to the irreversible adsorption of CO formed by decarbonylation as the analysis of the gas phase in the autoclave showed the presence of significant amounts of propane and propene that can only be obtained by decarbonylation of crotonaldehyde under the present reaction conditions. A comparison of the activity in gas and liquid phase showed that the catalysts lost their activity completely after a defined number of turnovers in the liquid phase, while they were still active after the same number of turnovers in the gas phase. This is attributed to the higher concentration of reactants and lower concentration of hydrogen on the catalyst surface in the liquid phase experiments.

The role of the side reaction leading to irreversibly adsorbed organic molecules (indicated by the bands at 2968, 2942, 2913, and 2882 cm^{-1}, see Fig. 6) remains unclear. These hydrocarbons, most probably formed by aldol condensation, dimerisation or condensation, were exclusively found when crotonaldehyde, hydrogen, and Pt were present. This in turn suggests that Pt plays an important role in the formation of these side products. It may be possible that the slow formation of these species at the surface and the slow change in selectivity to crotylalcohol are interrelated (21). For example, a layer of polymers is more dense on (111) planes than elsewhere and this would promote the adsorption of crotonaldehyde via the C=O bond. In this context, it is interesting to note that for other hydrogenation reactions a dependence of the selectivity on the concentration of carbonaceous layers on the metal was found (37).

4.3. Hydrogenation of Crotonaldehyde over Pt/TiO_2

The selectivities of Pt/SiO_2 and Pt/TiO_2 with similar particle sizes were nearly identical after reduction at 473 K. The selectivity to the unsaturated alcohol in the hydrogenation of crotonaldehyde in the gas phase increased with increasing particle size. While a selectivity of 11% to crotylalcohol was found for the catalyst with small particles, a selectivity of 41% was found for the catalyst with the largest particles (see Table 4). In accordance with observations in Refs. (1, 2), the activity and the selectivity to crotylalcohol increased significantly for Pt/TiO_2 catalysts after high-temperature reduction. We like to attribute this to the special state of titania in these catalysts.

The titania suboxides (TiO_x) decorating the Pt particles after reduction at high temperatures have coordinatively unsaturated Ti cations that may interact with electron pair

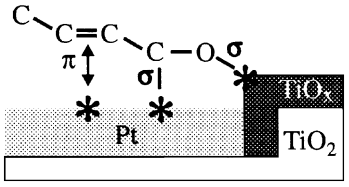

FIG. 11. Proposed sorption structure of crotonaldehyde on Pt/TiO_2 in the SMSI state.

donor sites. The strongest electron pair donor (of crotonaldehyde) is the oxygen of the carbonyl group. Thus, the carbonyl group is suggested to strongly interact with the Lewis acid sites (see Fig. 11). The coordination of a lone pair of electrons of oxygen to the electron deficient titania decreases the electron density of the C=O bond and, hence, increases its reactivity. Selective hydrogenation, thus, occurs if the sorption takes place close to the metal titania–suboxide interface where the carbonyl group can be activated by the Lewis site and dissociated hydrogen can be supplied by Pt. For catalysts with small and medium sized Pt particles, the increase in selectivity after reduction at 773 K is explained by the presence of this active interface.

For large Pt particles (C3), the increase in selectivity after reduction at 773 K (43%) compared with reduction at 473 K (41%) is low, because the fraction of active interface compared with the area of free metal surface is low. The selectivity of this catalyst is mainly determined by the relative abundance of the different surfaces of the Pt particles. The highest selectivity (64%) was observed for the catalyst with the largest particles after long reduction or reduction–oxidation–reduction cycles (Table 4). It seems that for large metal particles more time is required for the spreading of suboxides on the metal surface. The observed high selectivity is attributed to a high abundance of Pt(111) planes in combination with a significant fraction of Pt titania–suboxide interface. A selectivity of 100% seems difficult to reach, because the coordination of the π-electron system of the olefinic group (Fig. 11) to Pt can hardly be seen completely inhibited in such a scenario.

The highest activity (TOF) was observed after reduction between 673 and 773 K for all particle sizes (Fig. 9). As the rates of both the C=O and the C=C bond hydrogenation increased, one might speculate that the higher activity is caused by the creation of more active sites and/or by a lower rate of deactivation. In analogy to the silica supported catalysts, a fast deactivation was observed, especially during the first 15 min on stream. Our experimental results give no indication for a different rate or mechanism of deactivation after high-temperature reduction. Thus, it is unlikely that the difference in activity can be explained only by poisoning effects. However, it can be speculated that a change in the adsorption constant of crotonaldehyde at modified sites ($Pt–TiO_x$) due to, e.g., a change in the heat of adsorption may result in a higher turnover number per site and, thus, in a higher activity. When crotonaldehyde is strongly adsorbed at the $Pt–TiO_x$ interface, the rate of hydrogenation of the C=C bond may be enhanced, because of the geometric arrangement of crotonaldehyde as suggested in Fig. 11. The high activity seems to be specific for catalysts in the SMSI state. However, the rate of crotonaldehyde hydrogenation passes a maximum at reduction temperatures between 673 and 773 K and decreases with a further increase in reduction temperature (see Fig. 9). Higher reduction temperatures probably lead to a complete covering of the metal surface by a dense TiO_x overlayer and/or to an alloy formation with the reduced support (PtTi-alloy).

The selectivity to the unsaturated alcohol in the liquid phase increased with increasing metal particle size similar to the results obtained in the gas phase hydrogenation. The activity of the TiO_2-supported catalysts was also similar to the results obtained for silica supported catalysts in the liquid phase. The typical properties of TiO_x decorated catalysts were not observed in the liquid-phase studies probably due to the influence of moisture during the loading procedure of the autoclave reverting the SMSI state of the catalyst.

5. CONCLUSION

The hydrogenation of crotonaldehyde over Pt/SiO_2 and Pt/TiO_2 catalysts to the primary products butyraldehyde and crotylalcohol depends critically on the size of the Pt particles and the promotion by surface oxides. The selectivity is concluded to be directly controlled by the adsorption structure of crotonaldehyde. In the case of large particles, the prevalent dense Pt(111) surface planes of Pt constrain the sorption of the C=C double bond which enhances the selectivity to hydrogenate the C=O double bond. On small particles, the abundance of highly exposed metal atoms allows an unrestricted sorption of both double bonds. In this situation the hydrogenation of the C=C bond is favored.

With the metal oxide decoration of the Pt particles by titania suboxides (SMSI state) after high-temperature reduction, the presence of coordinatively unsaturated Ti cations strengthens the interaction of the catalyst with the C=O bond of crotonaldehyde and enhances the selectivity for the C=O bond hydrogenation. The particle size and the promotion by TiO_x are strictly additive effects and exert approximately the same effects upon the selectivity. In other words, TiO_x promotion on a catalyst with small particles and the presence of large particles allows to reach selectivities to crotylalcohol of approximately 45%. Promotion of large Pt particles with TiO_x oxides allows to reach a selectivity of 64%.

ACKNOWLEDGMENTS

We gratefully acknowledge the financial support of this work by the Christian Doppler Society. Research was carried out at the National Synchrotron Light Source, Brookhaven National Laboratory, which is

supported by the U.S. Department of Energy, Division of Materials Sciences and Division of Chemical Sciences.

REFERENCES

1. Vannice, M. A., and Sen, B., *J. Catal.* **115**, 65 (1989).
2. Vannice, M. A., *J. Mol. Catal.* **59**, 165 (1990).
3. Gallezot, P., Giroir-Fendler, A., and Richard, D., *in* "Catalysis of Organic Reactions" (W. Pascoe, Ed.), p. 1. Dekker, New York, 1991.
4. Coq, B., Figueras, F., Geneste, P., Moreau, C., Moreau, P., and Warawdekar, M., *J. Mol. Catal.* **78**, 211 (1993).
5. Marinelli, T. B. L. W., Vleeming, J. H., and Ponec, V., *in* "Proceedings, 10th International Congress on Catalysis, 1992," Budapest, "New Frontiers in Catalysis" (Guczi *et al.* Eds.), p. 1211. Elsevier, Amsterdam, 1993.
6. Richard, D., Ockleford, J., Girod-Fendler, A., and Gallezot, P., *Catal. Lett.* **3**, 53 (1989).
7. Richard, D., Foilloux, P., and Gallezot, P., *in* "Proceedings, 9th International Congress on Catalysis" (M. J. Phillips and M. Ternan, Eds.), Vol. 3, p. 1074. The Chemical Institute of Canada, Ottawa (1988).
8. Coq. B., Kumbhar, P. S., Moreau, C., and Warawdekar, M. G., *J. Mol. Catal.* **85**, 215 (1993).
9. Gallezot, P., Giroir-Fendler, A., and Richard, D., *Catal. Lett.* **5**, 169 (1990).
10. Galvagno, S., Capannelli, G., Neri, G., Donato, A., and Pietropaolo, R., *J. Mol. Catal.* **64**, 237 (1991).
11. Giroir-Fendler, A., Richard, D., and Gallezot, P., *Catal. Lett.* **5**, 175 (1990).
12. Delbecq, F., and Sautet, P., *J. Catal.* **152**, 217 (1995).
13. Beccat, P., Bertolini, J. C., Gauthier, Y., Massardier, J., and Ruiz, P., *J. Catal.* **126**, 451 (1990).
14. Van Hardeveld, R., and Hartog, F., *Surf. Sci.* **15**, 189 (1969).
15. Bond, G. C., and Wells, P. B., *Appl. Catal.* **18**, 225 (1985).
16. Matyi, R. J., Schartz, L. H., and Butt, J. B., *Catal. Rev.-Sci. Eng.* **29**(1), 41 (1987).
17. Jentys, A., Englisch, M., Haller, G. L., and Lercher, J. A., *Catal. Lett.* **21**, 303 (1993).
18. Jentys, A., McHugh, B. J., Haller, G. L., and Lercher, J. A., *J. Phys. Chem*. **96**, 1324 (1992).
19. Raab, C. G., and Lercher, J. A., *J. Mol. Catal.* **75**, 71 (1992).
20. Wanke, S. E., and Flynn, P. C., *Catal. Rev.-Sci. Eng.* **12**(1), 93 (1975).
21. Little, L. H., *in* "Infrared Spectra of Adsorbed Species," Academic Press, New York, 1966.
22. Englisch, M., Ranade, V. S., and Lercher, J. A., submitted for publication.
23. Kip, B. J., Duivenvoorden, F. B. M., Koningsberger, D. C., and Prins, R., *J. Catal.* **105**, 26 (1987).
24. Wang, L., Qiao, G. W., Ye, H. Q., Kuo, K. H., and Chen, Y. X., *in* "Proceedings, 9th International Congress on Catalysis," (M. J. Phillips and M. Ternan, Eds.), Vol. 3, p. 1253. The Chemical Institute of Canada, Ottawa (1988).
25. Dumesic, J. A., Stevenson, S. A., Sherwood, R. D., and Baker, R. T. K., *J. Catal.* **99**, 79 (1986).
26. Datye, A. K., Kalakkad, D. S., Yao, M. H., and Smith, D. J., *J. Catal.* **155**, 148 (1995).
27. Short, D. R., Mansour, A. N., Cook, Jr., J. W., Sayers, D. E., and Katzer, J. R., *J. Catal.* **82**, 299 (1983).
28. Vaarkamp, M., Thesis, University of Endhoven, The Netherlands (1993).
29. Vaarkamp, M., Miller, J. T., Modica, F. S., Lane, G. S., and Koningsberger, D. C., "Proceedings, 10th International Congress on Catalysis, 1992," Budapest, p. 809.
30. Englisch, M., Thesis, Univeristy of Twente, The Netherlands, 1996.
31. Hoare, M. R., and Pal, P., *Advan. Phys.* **20**, 161 (1971).
32. Ramachandran, A. S., Anderson, S. L., and Datye, A. K., *Ultramicroscopy* **51**, 282 (1993).
33. Van Santen, R. A., *Catal. Lett.* **16**, 59 (1992).
34. Gland, J. L., McClellan, M. R., and McFeely, F. R., *J. Vac. Sci. Technol. A* **1**, 1070 (1983).
35. Waghray, A., and Blackmond, D. G., *J. Phys. Chem*. **97**, 6002 (1993).
36. Eder, F., and Lercher, J. A., *J. Chem. Soc. Faraday Trans.* **90**(19), 2977 (1994).
37. Maetz, Ph., Saussey, J., Lavalley, J. C., and Touroude, R., *J. Catal.* **147**, 48 (1994).